Pergamon

Int. J. Heat Mass Transfer. Vol. 38, No. 8, pp. 1505–1515, 1995

0017-9310/95 $9.50+0.00

0017-9310(94)00257-6

Ice formation for turbulent flow in curved rectangular channels

J. BRAUN and H. BEER

Institut für Technische Thermodynamik, Technische Hochschule Darmstadt, Petersenstraße 30, 64287 Darmstadt, Germany

(*Received* 17 *March* 1994)

Abstract—The subject of this study is the ice formation at the cooled walls of a curved rectangular channel in case of turbulent flow. The steady state morphology of ice structure was investigated experimentally in two channels with different curvature. Even for moderately curved channels interactions between acceleration and centrifugal forces lead to significant differences in the morphology of the ice layers as compared to a straight channel. Additionally, a theoretical model was developed in order to describe the interaction of the different forces and their strong influence on the structure of turbulence. Numerically calculated ice layers are compared with experimental findings and a generally good agreement was found.

INTRODUCTION

Liquid solidification in pipes or channels is of interest in regions where the ambient temperature is below the freezing temperature throughout a long period of the year. In chemical engineering solidification might occur in many processes where cooling is required. Some of the resulting effects are desired (e.g. thermal insulation caused by the solid), some are unfavourable (e.g. in respect to an increase in pressure loss) and some must be avoided (pipe blockage and pipe breakage).

Ice formation in straight channels has been investigated in many previous works. For laminar flow one of the first theoretical models was developed by Zerkle and Sunderland [1]. Several other experimental as well as theoretical investigations followed for different geometries and/or boundary conditions [2–4]. The validity of those theories has been verified by experiments, e.g. for the parallel plate channel a very good experimental investigation of ice formation in laminar flow has been performed by Kikuchi [5].

Ice formation in turbulent flow shows a significant difference as compared to laminar flow because of the interactions between the ice layer development, which subsequently causes flow acceleration, and the structure of turbulence itself. Strong acceleration suppresses turbulence, a phenomenon which previously has been called 'laminarization' of the flow. Contrarily, when acceleration falls short of a critical value, 'retransition' to turbulent flow occurs and influences the development of the frozen crust. These interactions lead to waves in the ice layers which have been described in several experimental [6–9] and theoretical [9–11] investigations. However, as pipe systems do not only consist of straight ducts but contain curved sections as well, the consideration of curvature seems to be of practical importance. Despite this importance, ice formation in curved flow has so far been investigated only rarely. Laminar flow ice formation in curved tubes was described by Oiwake and Inaba [12]; Ichimiya and Shimomura [13] showed similar results for a rectangular channel. Ice formation in turbulent flow has been investigated by Fukusako [14] for the case of asymmetrically cooled channels where either the convex or the concave wall was cooled, while the opposite wall was adiabatic.

The present study is concerned with a detailed investigation of the ice formation phenomena in turbulent flow in a curved rectangular channel with both curved walls cooled. As compared to the straight channel there are significant differences even if the rate of curvature is small (i.e. $4h/R_m \approx 0.1$). The ice layers are asymmetric and clearly show the different influence which curvature has on turbulence near a concave and a convex wall, respectively. A very detailed description of the effects of curvature on turbulent flow was presented by Bradshaw [15].

EXPERIMENTS

Figure 1 shows the experimental apparatus which consists of the test section, a circuit for the coolant (which is a mixture of 30% ethylene glycol and water) and the circulating system for the test liquid (water). The temperature of the coolant is held constant by constant cooling with the aid of a refrigeration unit and by simultaneous variable heating. The power supply of the resistance heating is controlled by a temperature dependant resistor (NTC). This arrangement results in fluctuations of the mean temperature of less than 0.05 K for steady state conditions.

The flow rate of the water is measured with a calibrated venturi nozzle which is installed behind the centrifugal pump and the control valve. Behind a

NOMENCLATURE

a	thermal diffusivity
B	freezing parameter, $(k_s/k_l)(T_f-T_w)/(T_0-T_f)$
c	heat capacity
d_h	hydraulic diameter, $4h$
h	half channel height
K	dimensionless pressure gradient
$\mathscr{K}$	ratio of acceleration to centrifugal force
k	thermal conductivity
l	ice layer thickness or mixing length, respectively
p	pressure
$\dot{q}$	heat flux density
R	radius
r, φ	coordinates
Re_{4h}	Reynolds number $(4Re_h)$, $(\overline{w_0}4h/\nu)$
Ri	Richardson number, $\{(\bar{u}_\varphi/r)/[(\partial\bar{u}_\varphi/\partial r)-(\bar{u}_\varphi/r)]\}$
T	temperature
u_r, u_φ	velocity components
$\overline{w_0}$	mean axial velocity
x	axial distance (center line)
y	rectangular distance from center line, $r-R_i$.

Greek symbols

γ	channel curvature
δ	half span between ice layers
ε	eddy viscosity
Θ_c	cooling parameter, $(T_f-T_w)/(T_0-T_f)$
ν	kinematic viscosity
ξ	weight function
ρ	density
τ	shear stress
ψ	stream function.

Subscripts

0	at entrance
a	concave wall
f	at freezing temperature
i	convex wall
l	liquid
m	channel center line
s	solid
t	turbulent
w	wall
∞	outside boundary layer.

Superscripts

$\overline{(\cdots)}$	time mean value
$(\cdots)'$	time dependant value
$(\cdots)^+$	wall coordinates.

calming section, build in to obtain a fully developed turbulent flow, the water enters the test section. The mean temperature of the water is soon measured in front of and behind the test section. The inlet water temperature is controlled with a similar facility as the coolant temperature and the fluctuations are less than 0.02 K for steady state conditions.

Both test sections have a cross-section of 24 mm × 100 mm. The radius of curvature of the moderately curved channel is 495 mm while that of the strongly curved channel is 112 mm. The temperatures at the water side surfaces of the cooled plates are measured with the help of calibrated chromel–alumel thermocouples. The deviation of the measured wall

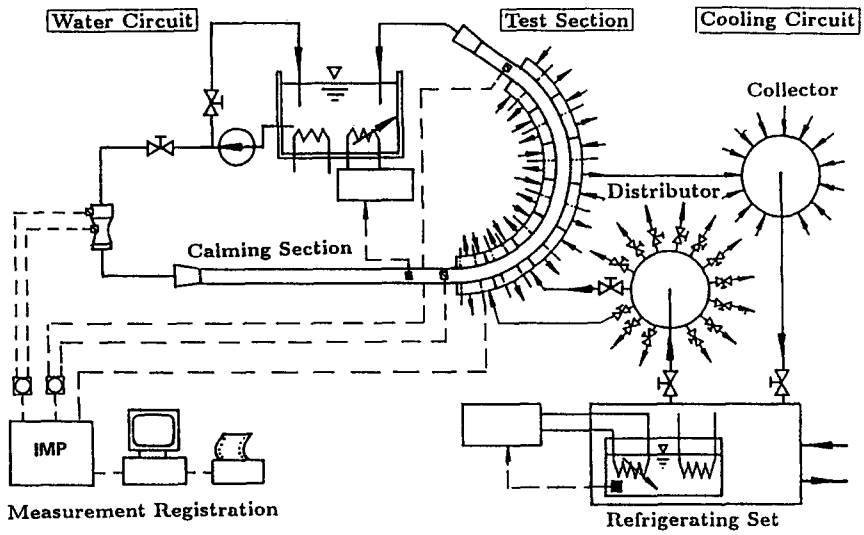

Fig. 1. Experimental apparatus.

temperatures from the mean value was in all cases less than 0.3 K, normally less than 0.15 K.

All data are recorded after steady state conditions are achieved. The thickness of the ice layer is measured by means of a microscope with an accuracy of 0.1 mm. Additionally, a photographic registration of the ice layers is performed. To give a better contrast, the dye methylene blue is added to the water. This does not cause any change of the physical properties within the limits of accuracy.

The experiments were performed in the following ranges of the Reynolds number and the cooling parameter: $9000 < Re_{4h} < 47\,000$ and $1 < \Theta_c < 18$.

EXPERIMENTAL OBSERVATIONS

In a straight channel Seki [8] and Weigand [9] have both observed basically four different forms of ice layers. At the lowest values of the cooling parameter Θ_c ice layers are smooth and no laminarization of the flow is observed. With an increase in Θ_c effects of laminarization and retransition of the turbulent flow become visible by an increasing variety of waves, without or with separation of the flow. Previously, the forms of ice layers were designated as the smooth transition, step transition and the wavy ice layers. With the exception of the wavy ice layers, which are unstable, the other forms were symmetric to the center line of the channel (see refs. [8, 9]).

In a curved channel the ice layers are never symmetric because of the completely different behaviour of turbulence near a convex and a concave wall. Because of this different behaviour, a new form of ice formation has been found in the experiments where the ice layer at the concave wall remains smooth while at the convex wall flow separation occurs and leads to a step change in ice layer thickness. In the following this form will be called the 'mixed transition ice layer'.

In a curved channel an increase in cooling parameter Θ_c at a constant Reynolds number results in the following ice formations.

Smooth ice layers. At the lowest values of Θ_c, ice layers grow monotonically from the entrance of the curved channel and attain a nearly constant thickness downstream. No effects of laminarization are detectable and the ice layers remain smooth. At the convex wall they are slightly thicker than at the concave wall [Fig. 2(a)]. Smooth ice layers are comparatively thin and, because of a negligible acceleration of the flow in the entrance region, they can be calculated with the help of a modified mixing length model, described later.

Smooth transition ice layers. The second type are the smooth transition ice layers which, at both walls, increase in thickness from the entrance of the channel until they reach a maximum value. Behind that point ice layer thickness decreases gradually until it again attains a nearly constant value [Fig. 2(b)].

As a result of a higher freezing parameter the flow passage converges and the acceleration of the flow in

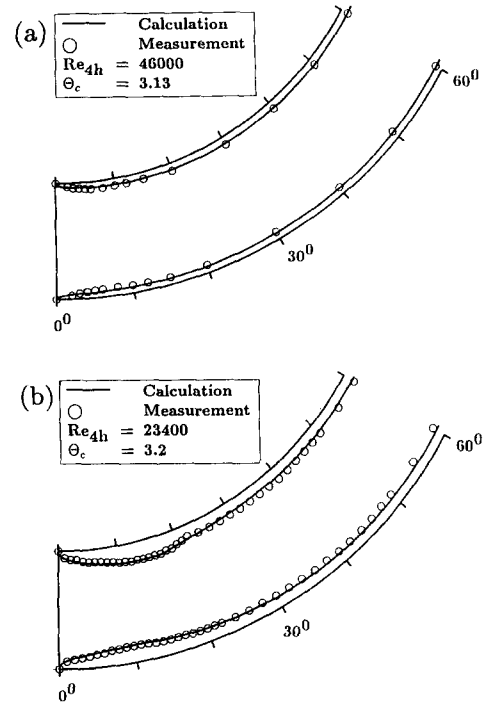

Fig. 2. (a) Smooth ice layer; (b) smooth transition ice layer.

the entrance region is strong enough to suppress the turbulent motion and to laminarize the flow. Especially the ice layer thickness at the convex wall exceeds values which would be predicted for fully developed turbulent flow. Some hydraulic diameters downstream, the acceleration recedes and the flow is enabled to return to its originally turbulent state. This enhances heat transfer and the ice layer thickness begins to decrease. At the concave wall this enhancement is more pronounced than at the convex wall or at a straight wall.

At the convex wall turbulent motion is suppressed by centrifugal forces and by acceleration so that at this side of the channel laminarization due to acceleration and suppression of the turbulent motion due to curvature are superimposed. This results in a thicker ice layer which can be observed in Fig. 2(b). At the point, however, where the free channel height begins to increase, turbulent motion is enhanced also at the inner (convex) wall and the ice layer thickness decreases. In this region the solid crust forms a diffuser with a small angle so that flow separation does not occur.

Mixed transition ice layers. A very interesting ice formation is presented with the third domain because it accentuates the influence of curvature with regard to the different behaviour of the flow at the convex and the concave wall, even for small curvatures. Due to the higher rate of laminarization (higher value of the cooling parameter) the reactivation of the turbulent motion at the convex wall sets in more intensively than in the preceding case. Additionally, the slope of the velocity profile near a convex wall is

somewhat smaller than near a straight wall or a concave wall so that the resulting fast decrease of the ice layer thickness leads to flow separation at this point and a step is formed in the ice layer [Fig. 3(a)]. At the concave wall ice layer thickness starts to decrease further upstream and thus more gradually, and no separation of the flow is detected. Moreover, velocity gradients are steeper at concave walls than at straight or convex walls and, therefore, flow separation is impeded additionally. As compared to the observations in a straight channel, flow separation at the convex wall starts at slightly lower values of Θ_c while at the concave wall separation occurs at higher values of the freezing parameter (see next paragraph).

Step transition at both walls. A further increase in the cooling parameter leads to flow separation at both walls. At the concave wall the step in the ice layer develops further downstream as compared to that at the convex wall [Fig. 3(b)], and seems to be induced by flow separation at the convex wall. The asymmetry of the ice layers is more pronounced at low Reynolds numbers.

Wavy ice layers. If the cooling parameter Θ_c is increased again, more than one ice wave is obtained. The experiments show that the flow becomes unstable at high Reynolds numbers. Downstream of the first nearly symmetric step transition zone, a three-dimensional morphology develops (Fig. 4). Separation zones occur arbitrarily and do not span the whole width of the channel. In contrast to this instability the situation is different at low Reynolds numbers, $Re_{4h} < 15\,000$. Wavy ice layers occur already in the mixed transition regime and have a rather periodic shape. Flow separation occurs only at the convex wall, while the ice layer at the concave wall still remains smooth (Fig. 5). The waves downstream are similar to the first one and are two-dimensional. Because of the regular shape of the steps, the mechanism of their development is believed to be a periodic repetition of the acceleration effect which leads to the first wave rather than instability of the flow.

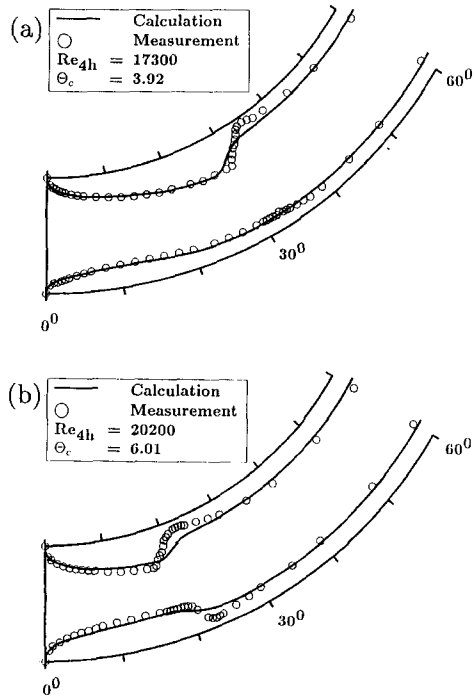

Fig. 3. (a) Mixed transition ice layer; (b) step transition ice layer.

CLASSIFICATION OF THE ICE LAYERS

The ice layers can be classified with the aid of a Θ_c–Re_{4h}-diagram which was proposed by Gilpin [6] and used by Seki [8] and Weigand [9] for a straight channel. The diagram for the moderately curved channel is depicted in Fig. 6.

The different types of ice layers are marked by different symbols and the dashed lines, separating the different regimes in a straight channel (see Weigand [9, 11]), are added for comparison. As compared to those of the straight channel, the slope of the separation lines for a curved channel is smaller. This indicates that retransition generally occurs at lower values of the cooling parameter Θ_c if curvature acts additionally on the flow. In a curved channel ice layers show significant differences at the concave and the convex wall, respectively. The border line between the zone of smooth and mixed transition is the line of flow separation incipience at the convex wall and lies below that of the straight channel. Looking at the line indicating flow separation at the concave wall, one observes that this line lies above that of the straight channel, with the exception of higher Reynolds numbers. This observation shows that flow separation is suppressed by concave curvature and is enhanced by convex curvature.

All observed ice layers can be explained rather easily in a qualitative way by the interaction of only two essential flow phenomena:

(i) the strong acceleration of the flow in the entrance region of the test section, caused by the growing ice layers, suppresses the turbulent motion (laminarization, see Deissler [17, 18]) and leads to a further increase in ice layer thickness;

(ii) stream line curvature has, depending on the sign of curvature, two opposite effects: at the convex wall turbulent motion in the radial direction is suppressed, whereas it is enhanced at the concave wall. Basically, this yields higher slopes of the velocity and the temperature profile at the concave wall, and explains the observation that flow separation is suppressed and heat transfer is enhanced. The explanation for the behaviour at the convex wall is vice versa.

COMPARISON BETWEEN THE ICE LAYERS IN A STRAIGHT AND THE CURVED CHANNELS

The effects of curvature on ice formation become obvious when ice layers in a straight channel are com-

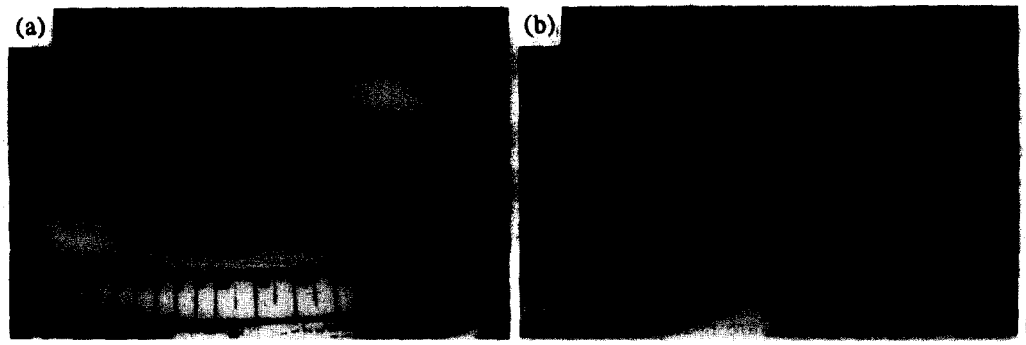

Fig. 4. Irregular wavy ice layer at $Re_{4h} = 45\,954$ and $\Theta_c = 11.8$: (a) $\varphi = 0° \ldots 24°$ (b) $\varphi = 72° \ldots 96°$.

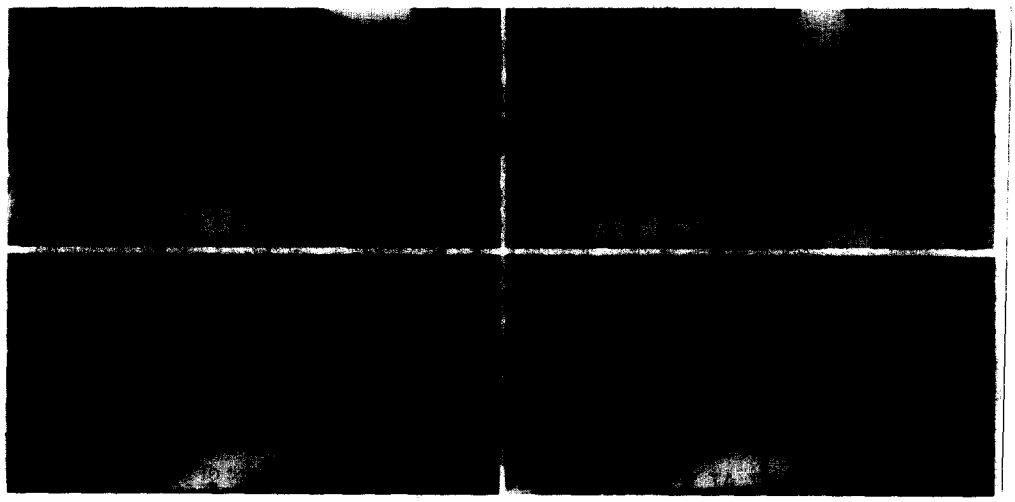

Fig. 5. Periodic wavy ice layer at $Re_{4h} = 12\,420$ and $\Theta_c = 3.3$.

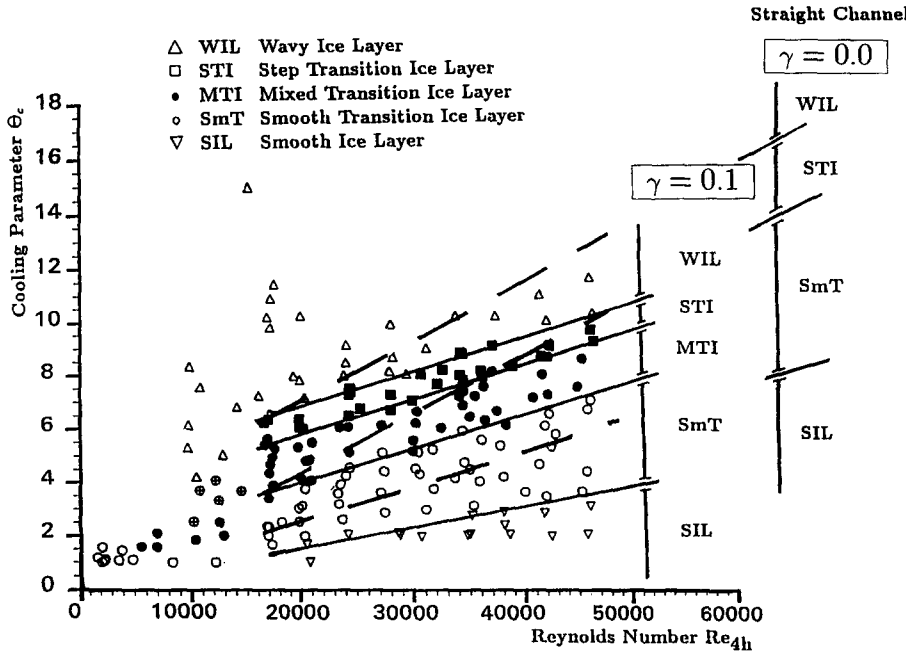

Fig. 6. Classification of ice structures in the Θ_c–Re_{4h}-diagram ($\gamma = 0.1$).

pared with those in the moderately curved and the strongly curved channel. Figure 7 shows three ice layers recorded at $Re = 20\,500$ and at a cooling parameter $\Theta_c = 4$. The ice layer in the straight channel was determined by Weigand [9] and classified as a smooth transition ice layer while both ice layers in the curved channels belong to the mixed transition regime.

In the entrance region of both curved channels, the ice layers at the convex walls are thicker than the ice layer at the straight wall and are nearly identical in shape. From the channel entrance up to the separation zone they match well with ice layers calculated for *laminar* flow. This shows that, even for a moderately curved channel ($\gamma = 0.1$), acceleration and convex curvature together suppress turbulence almost perfectly and that even stronger curvature ($\gamma = 0.43$) does not intensify this effect. At the concave wall, however, acceleration and concave curvature have an opposite effect on turbulent motion. Acceleration suppresses while concave curvature enhances turbulence. This is elucidated by Fig. 7, showing that retransition to turbulent flow starts further upstream with increasing curvature. In the straight channel retransition is observed at $x/h \approx 15$, in the moderately curved channel at $x/h \approx 9$ and in the strongly curved channel at $x/h \approx 3.5$. As will be shown, this interaction between acceleration and curvature can be used to determine the retransition point at the concave wall theoretically.

THE RETRANSITION POINT AT THE CONCAVE WALL

In a straight channel Gilpin [6], Seki [8] and Weigand [9] used a dimensionless pressure gradient to determine the retransition from the laminarized to the fully turbulent flow which has been defined by Moretti and Kays [19]:

$$K = \frac{\nu}{\rho(u_\infty)^3}\frac{\partial p}{\partial x}. \tag{1}$$

For the curved channel this equation can be transformed to

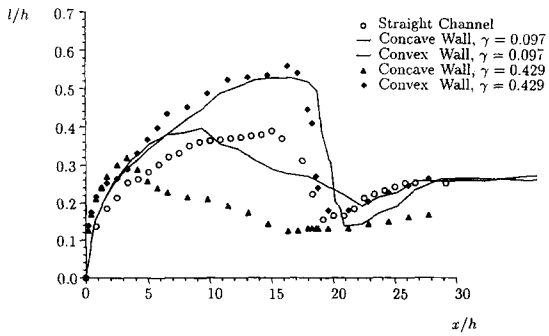

Fig. 7. Comparison of ice layers in curved and straight channels.

$$K = -\frac{1}{Re_h R_m}\frac{\partial \delta}{\partial \varphi}. \tag{2}$$

If the pressure gradient (induced by the acceleration of the flow) falls below a critical value turbulent motion might start (instability point). Moretti and Kays [19] and Narasimha and Sreenivasan [20] found slightly different values for a possible onset of turbulent motion. However, the instability criterion is within the range

$$K_{crit} \in [2 \times 10^{-6} - 3.5 \times 10^{-6}]. \tag{3}$$

In a straight channel one can observe that the actual point of retransition lies somewhat downstream of the instability point and the difference between those two locations was determined by Seki [8] and Weigand [9] with the help of an empirical formula.

At the concave wall of a curved channel the point of retransition can be determined with high accuracy with the following consideration. Retransition will occur when the ratio of the acceleration force to the centrifugal force falls below a critical value, i.e.

$$\mathscr{K} = \frac{w\dfrac{dw}{dx}}{\dfrac{w^2}{R}} = \frac{-\dfrac{w^2}{\delta}\dfrac{d\delta}{dx}}{\dfrac{w^2}{R}} = -\frac{R}{\delta}\frac{d\delta}{dx} = -\frac{1}{\delta}\frac{d\delta}{d\varphi} < \mathscr{K}_{crit}. \tag{4}$$

As a first approximation $\mathscr{K}_{crit}$ can be estimated to be 1, which means that retransition occurs if acceleration and centrifugal forces are of the same order of magnitude. The actual critical value, however, was obtained from the experiments at the location where the ice layers at the convex and the concave wall begin to diverge, which is shortly in front of the point of maximum ice layer thickness at the concave wall; see Fig. 8(a). It was found that $\mathscr{K}_{crit}$ is independent of the flow Reynolds number but that there is a linear dependance on the cooling parameter Θ_c [Fig. 8(b)]. The linear dependance on Θ_c holds for the moderately as well as for the strongly curved channel, but with a different slope. This requires an additional dependance on the radius of curvature of the channel and finally the critical value $\mathscr{K}_{crit}$ becomes

$$\mathscr{K}_{crit} = 0.0495\Theta_c \gamma^{-0.75} \tag{5}$$

where

$$\gamma = d_h/R_m. \tag{6}$$

With this equation the instability point at the concave wall can be determined easily.

ANALYSIS

The theoretical investigation which will be outlined briefly can be separated into two parts, the simplification of the conservation equations and the modelling of the turbulent quantities.

The boundary conditions and the geometry of the

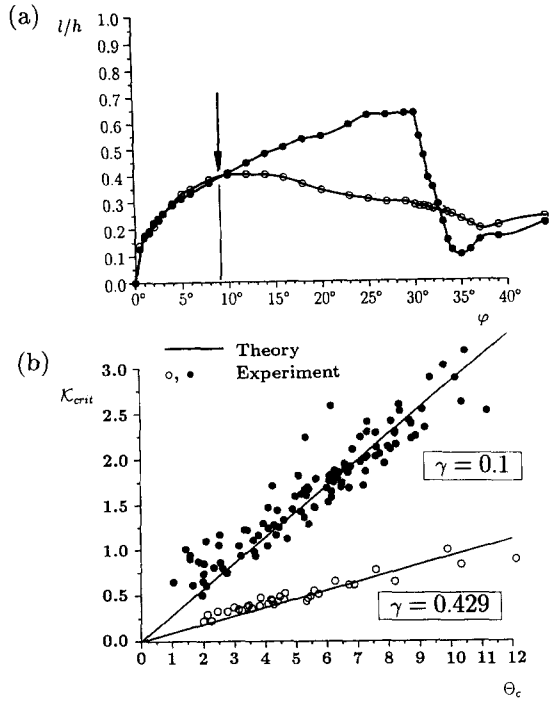

Fig. 8. (a) Retransition point at the concave wall (from experiments); (b) dependance of $\mathcal{K}_{crit}$ on the cooling parameter Θ_c and on the curvature γ.

test sections used for the experimental investigation lead to the assumption that the flow is two-dimensional. This has been confirmed by several investigations of turbulent flows in curved rectangular channels (e.g. see refs. [22–24]). Furthermore, the analysis is based on the assumption of an incompressible, Newtonian fluid with constant properties k, c, ρ and η, and steady state conditions are presumed. Figure 9 shows the geometry of the channel under consideration. As usual for the theoretical treatment of turbulent flows, the quantities of the flow field are split into their time mean and time dependent value, and because of an assumed large curvature radius the common boundary layer approximation can be used [15]. With these assumptions the conservation equations for mass, momentum and energy can be written as follows:

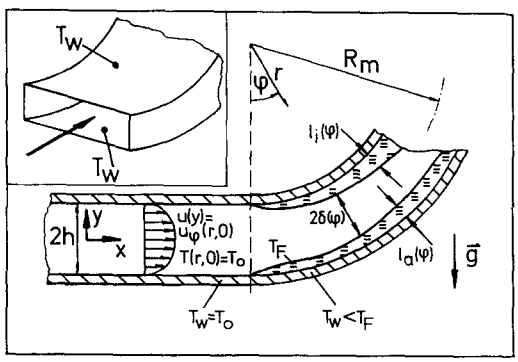

Fig. 9. Geometry of the channel.

Continuity equation:

$$\frac{1}{r}\frac{\partial(\bar{u}_r r)}{\partial r}+\frac{1}{r}\frac{\partial \bar{u}_\varphi}{\partial \varphi}=0. \tag{7}$$

Conservation of momentum in r-direction:

$$\frac{\bar{u}_\varphi^2}{r}=\frac{1}{\rho}\frac{\partial P}{\partial r}. \tag{8}$$

Conservation of momentum in φ-direction:

$$\bar{u}_r\frac{\partial \bar{u}_\varphi}{\partial r}+\frac{\bar{u}_\varphi}{r}\frac{\partial \bar{u}_\varphi}{\partial \varphi}=-\frac{1}{\rho r}\frac{\partial P}{\partial \varphi}+\frac{1}{r^2}\frac{\partial}{\partial r}\left\{r^2\left(\nu r\frac{\partial}{\partial r}\left[\frac{\bar{u}_\varphi}{r}\right]-\overline{u_r' u_\varphi'}\right)\right\}. \tag{9}$$

Conservation of energy for the liquid:

$$\bar{u}_r\frac{\partial \bar{T}}{\partial r}+\frac{\bar{u}_\varphi}{r}\frac{\partial \bar{T}}{\partial \varphi}=\frac{1}{r}\frac{\partial}{\partial r}\left[r\left(a\frac{\partial \bar{T}}{\partial r}-\overline{T' u_r'}\right)\right]. \tag{10}$$

Conservation of energy for the solid:

$$\frac{a_s}{r}\frac{\partial}{\partial r}\left(r\frac{\partial T_s}{\partial r}\right)=0. \tag{11}$$

The static pressure $\bar{p}$ and the shear stress τ_{rr} are combined in the new quantity P with $P=\bar{p}+\tau_{rr}$.

Boundary conditions and interface energy equation

To solve the partial differential equations the following boundary and initial conditions for the liquid and the solid are used:

$$\varphi=0:\quad \bar{u}_r=0;\quad \bar{u}_\varphi, P \text{ given};\quad \bar{T}=T_0 \tag{12}$$

$r=R_i+l_i\cong R_m-\delta$ and $r=R_a-l_a\cong R_m+\delta$:

$$\bar{u}_\varphi=0,\quad \bar{T}=T_s=T_f \tag{13}$$

and additionally for the solid phase:

$$r=R_i \text{ and } r=R_a:\quad T_s=T_w. \tag{14}$$

At the solid liquid interface (i.e. $r=R_i+l_i$ and $r=R_a-l_a$) conservation of energy leads to a relation between the radial temperature gradients in the liquid and the solid. Steady state conditions provided, the heat flux from the liquid to the solid must equal the heat flux from the solid to the wall. This condition may be written in terms of the temperature gradients:

$$k_s\frac{\partial T_s}{\partial r}=k_l\frac{\partial \bar{T}}{\partial r}. \tag{15}$$

Coordinate transformation and dimensionless quantities

After the introduction of a stream function ψ which is defined

$$\bar{u}_\varphi=\frac{\partial \psi}{\partial r};\quad \bar{u}_r=-\frac{1}{r}\frac{\partial \psi}{\partial \varphi} \tag{16}$$

the equations are cast into a dimensionless form by dividing all variables by an appropriate combination of the quantities $\overline{w_0}$, h, $\sqrt{Re_h}$, ρ and (T_0-T_f) and are

solved numerically using the Keller–Box-method (see ref. [25]).

MODELLING OF THE TURBULENT QUANTITIES

The purpose of this chapter is the development of a turbulence model to describe the combined action of acceleration and curvature on the turbulent quantities. As already pointed out, turbulence in a curved channel with solidification at the walls is affected by (i) strong acceleration of the flow due to the growing ice layer, (ii) the stabilizing effect of curvature at the convex wall and (iii) the destabilizing effect of curvature at the concave wall. The representation of a mixed transition ice layer in a curved channel (Fig. 10) shows four different zones where the above-mentioned forces have a different influence on the ice formation.

Zone I. In the entrance region (I) of the cooled test section acceleration of the flow is predominant. Curvature of the wall has almost no influence on the structure of turbulence because acceleration forces are significantly higher. Narasimha and Sreenivasan [20] showed that turbulent motion in the axial (φ) direction is suppressed by strong acceleration forces. From theoretical considerations Deissler [17, 18] developed a turbulence model for highly accelerated flows and showed that the Reynolds shear stress and the turbulent heat flux are nearly constant for a constant value of the stream function ψ:

$$\overline{u_r' u_\varphi'}(\psi) = \overline{u_r' u_\varphi'}(\psi)|_0 \tag{17}$$

and

$$\overline{u_r' T'}(\psi) = \overline{u_r' T'}(\psi)|_0. \tag{18}$$

The critical value indicating strong acceleration was defined by Moretti and Kays [19] and is given by the equations (2) and (3). The actual acceleration of the flow at the entrance of the channel, however, is about one or two orders of magnitude higher and, therefore, equation (17) holds almost exactly in zone I.

Zone IV. In zone IV the acceleration of the flow is negligibly small and thus the effects of curvature prevail. The Reynolds shear stress $-\rho\overline{u_r' u_\varphi'}$ and the turbulent heat flux $-\rho c\overline{T' u_r'}$ are related to the mean quantities of the flow by an eddy viscosity concept:

$$\tau_t = -\rho\overline{u_r' u_\varphi'} = \rho\varepsilon_t r \frac{\partial}{\partial r}\left(\frac{\bar{u}_\varphi}{r}\right) \tag{19}$$

$$\dot{q}_t = -\rho c\overline{T' u_r'} = k_t \frac{\partial \bar{T}}{\partial r} = \rho c a_t \frac{\partial \bar{T}}{\partial r}. \tag{20}$$

The turbulent thermal diffusivity is calculated from the turbulent Prandtl number

$$Pr_t = \varepsilon_t / a_t \tag{21}$$

with Pr_t as proposed by Kays [21]:

$$Pr_t = \begin{cases} 1.43 - 0.17(y^+)^{0.25} & \text{if } Pr_t > 0.85 \\ 0.85 & \text{otherwise.} \end{cases} \tag{22}$$

For the fully developed turbulent flow a modified mixing length model is applied. To consider the effects of curvature Bradshaw [15] suggested the variation of the mixing length by a function of the Richardson number. For the turbulent shear stress this yields

$$\tau_t = -\rho\overline{u_r' u_\varphi'} = \rho l^2 \left| r\frac{\partial}{\partial r}\left(\frac{\bar{u}_\varphi}{r}\right)\right| r\frac{\partial}{\partial r}\left(\frac{\bar{u}_\varphi}{r}\right) \tag{23}$$

with the mixing length l:

$$\frac{l}{h} = \frac{l}{l_0}\frac{l_0}{h} = [1 - \beta Ri]^n \left[1 - \exp\left(-\frac{y}{A}\right)\right]$$

$$\times \left[0.14 - 0.08\left(1 - \frac{y}{h}\right)^2 - 0.06\left(1 - \frac{y}{h}\right)^4\right]. \tag{24}$$

The constant β in this equation has been determined to match the experimental findings of Wattendorf [22], Eskinazi and Yeh [23] and Kobayashi [24], resulting in

$$\beta = \begin{cases} 0.5 & \text{at the convex wall} \\ 20 & \text{at the concave wall.} \end{cases} \tag{25}$$

The different value of β at the convex and the concave wall, respectively, is called "zonal modelling" (see Muck *et al.* [16]). The exponent n is found by a theoretical consideration, yielding

$$n = \tfrac{1}{2}. \tag{26}$$

Zones II *and* III. In the intermediate zones II and III the reactivation of the turbulent motion has to be determined taking into account the different behaviour at the concave and the convex wall.

Behind the point of retransition at the concave wall turbulent motion at the convex wall is further suppressed by the centrifugal forces. This is visualized by Fig. 8(a) as a different development of the ice layer thickness at the inner and the outer wall. If a fluid particle near the convex wall is displaced radially into a region where the local radial pressure gradient is higher than the centrifugal force of the particle, it will be forced back to its original location. This behaviour

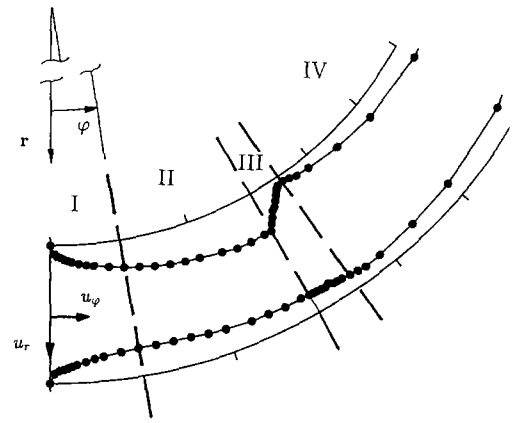

Fig. 10. Four zones of different influence on turbulent motion in a curved channel.

can be expressed in terms of the Richardson number as a result of a stability consideration in the radial direction which yields

$$1+2Ri\begin{cases}<0 & \text{and} \quad >1 \quad \text{for stability} \\ >0 & \text{and} \quad <1 \quad \text{for instability.}\end{cases} \tag{27}$$

When the flow gets unstable because of ceasing acceleration, the turbulent motion recovers rapidly in axial direction. The onset of the turbulent motion in axial direction is described analogously to the transition from laminar to turbulent flow and has the form of an exponential function of the axial coordinate φ.

The total turbulent shear stress in the transitional regions II and III is described as a transition from the Deissler shear stress in zone I, equation (17), to the mixing length value in zone IV, equation (23), with the help of a weight function ξ

$$\overline{u_r'u_\varphi'} = \xi \cdot \overline{u_r'u_\varphi'}|_{\text{Deissler}} + (1-\xi) \cdot \overline{u_r'u_\varphi'}|_{\text{mixing length}} \tag{28}$$

with

$$\xi = \exp(-C\varphi^2) \times f(1+2Ri) \tag{29}$$

(see Braun [26, 27]), where f is a function of $(1+2Ri)$ with a value between 0 and 1. In stable regions [see equation (27)] f equals 1.

Equation (28) takes into account the transition from laminarized to turbulent flow in axial direction as well as the suppression of turbulence near the convex wall and enhancement of turbulence near the concave wall. Figure 11 shows the weight function which has been calculated for a typical flow field of a mixed transition ice layer. With the help of the described theoretical model a computer program was developed to solve the partial differential equations numerically and to compare the results of the theoretical model with measured ice layers.

In case of flow separation and recirculation in zone III, the FLARE approximation (see ref. [28]) is applied additionally in order to get the calculation numerically stable. This approximation presumes that the transport terms in axial direction in the momentum and the energy equation are negligible in regions of recirculation where the axial velocity component is negative.

RESULTS AND DISCUSSION

The calculated ice layers are in good agreement with the measured values in all four zones of the channel, placing confidence in the theoretical model. Results of the numerical calculations of a smooth ice layer and a smooth transition ice layer are depicted in Fig. 2(a) and (b). Even for mixed and step transition ice layers the numerical analysis and the experiments compare quite well [Fig. 3(a) and (b)].

Because of the asymmetry due to curvature, mixed transition ice layers are very appropriate to demonstrate the effects of curvature and, therefore, a comparison between a calculated and a measured mixed transition ice layer will be discussed in more detail. Figure 12(a) shows the same ice layer as in Fig. 3(a). This representation is more suitable to compare the calculation and the measurement in the four different zones of the channel.

In zone I ($0 \leqslant x/h \leqslant 7.5$), where the ice layer is calculated with the help of the Deissler model, the agreement between theory and experiment is excellent. This shows clearly the strong laminarization of the flow caused by acceleration. In the experiment retransition at the concave wall occurred at $x/h \approx 7$. This is in very good agreement with the calculated value $x/h \approx 7.5$ from the retransition criterion in the curved channel, equation (5).

In zone II, which is defined up to the maximum ice layer thickness at the convex wall, theory and experiment are in a reasonably good agreement

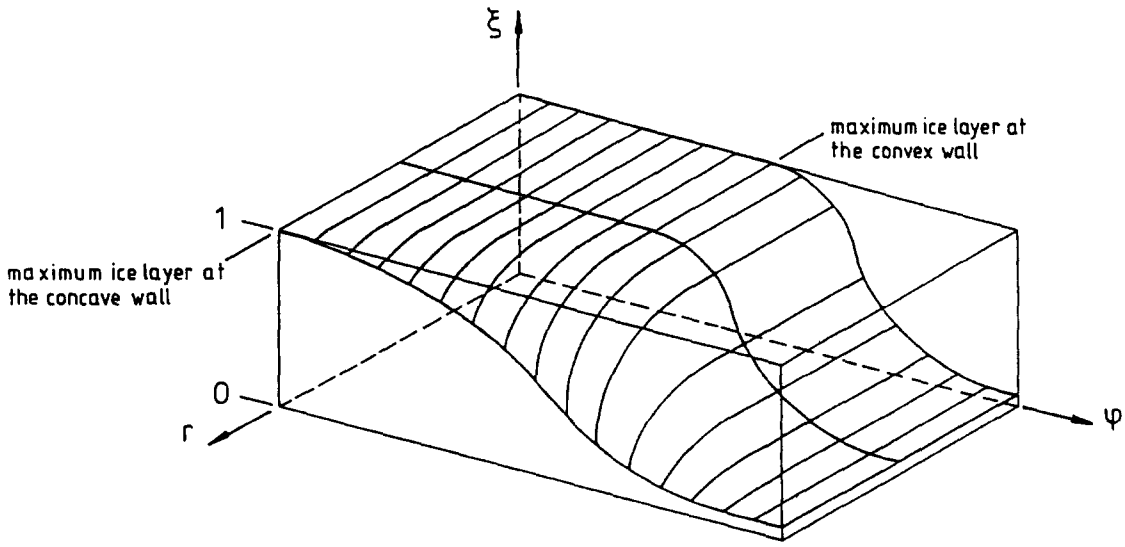

Fig. 11. Weight function ξ of the Deissler shear stress.

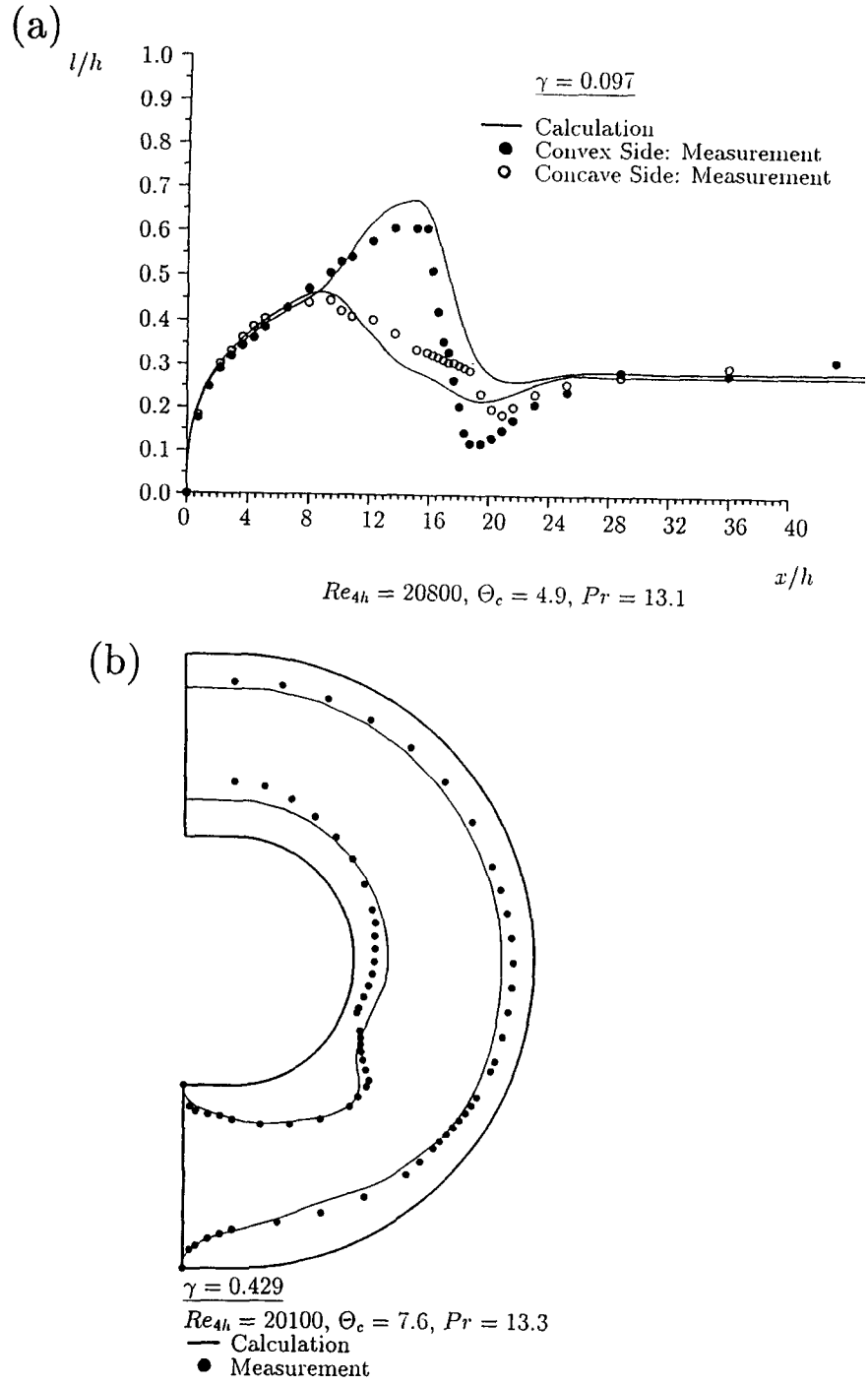

Fig. 12. Calculated mixed transition ice layers: (a) moderate curvature, (b) strong curvature.

($7.5 \leqslant x/h \leqslant 15.5$). In zone III ($15.5 \leqslant x/h \leqslant 20.5$), where flow separation occurs at the convex wall, the agreement between theory and experiment is rather poor. Especially, the deviation between the calculated and the measured values of minimum ice layer thickness is conspicous. This shows that further work has to be done on the theoretical modeling. In the last zone IV of the channel ($x/h \geqslant 20.5$), where acceleration is comparatively small as compared to the centrifugal forces, the flow behaviour is modeled very accurately with the aid of the Richardson model and the deviations between theory and experiment are again very small.

Generally, it can be pointed out that the results of the experiment and the numerical analysis are in good agreement for the moderately curved channel.

Finally, a comparison between a calculated and a measured ice layer for the strongly curved channel

($\gamma = 0.429$) is presented in Fig. 12(b). The plot again shows a very good agreement for zones I and II. In zone III the agreement is comparable to that in the moderately curved channel, whereas the coincidence is rather bad in zone IV. This shows that the mixing length model, modified for curved flows by the Richardson number, is no longer valid for strongly curved channels and that additional effects, such as large scale eddies, influence the turbulent quantities.

SUMMARY

The measurement of the ice layer thickness in a curved rectangular channel leads to the conclusion that there exist four zones with a different influence on the forces acting on the turbulent motion. These are the entrance zone of the cooled channel where acceleration is predominant and any influence of wall curvature can be neglected, a zone where centrifugal forces and flow acceleration are of the same order of magnitude and retransition is enhanced by instability at the concave wall, a zone where flow separation may occur and finally a region where the flow is almost only affected by stream line curvature.

Acknowledgement—The support of this work by the Deutsche Forschungsgemeinschaft is gratefully acknowledged.

REFERENCES

1. R. D. Zerkle and J. E. Sunderland, The effect of liquid solidification in a tube upon laminar-flow heat transfer and pressure drop, *J. Heat Transfer* **90,** 183–190 (1968).
2. D. G. Lee and R. D. Zerkle, The effect of liquid solidification in a parallel plate channel upon laminar-flow heat transfer and pressure drop, *J. Heat Transfer* **91,** 583–585 (1969).
3. B. Weigand and H. Beer, Heat transfer and solidification of a laminar liquid flow in a cooled parallel plate channel: the stationary case, *Wärme- und Stoffübertragung* **26,** 233–240 (1991).
4. B. Weigand and H. Beer, Transient freezing of liquids in forced laminar flow inside a parallel plate channel, *Wärme- und Stoffübertragung* **27,** 77–84 (1992).
5. Y. Kikuchi, Y. Shigemasa, A. Oe and T. Ogata, Steady state freezing of liquids in laminar flow between two parallel plates, *J. Nucl. Sci. Technol.* **23,** 979–991 (1986).
6. R. R. Gilpin, Ice formation in a pipe containing flows in the transition and turbulent regimes, *J. Heat Transfer* **103,** 363–368 (1981).
7. T. Hirata and H. Matsuzawa, A study of ice-formation phenomena on freezing of flowing water in a pipe, *J. Heat Transfer* **109,** 965–970 (1987).
8. N. Seki, S. Fukusako and G. Younan, Ice-formation phenomena for water flow between two cooled parallel plates, *J. Heat Transfer* **106,** 498–505 (1984).
9. B. Weigand, Erstarrungsvorgänge einer strömenden Flüssigkeit in einem ebenen, geraden Kanal, Doctoral Thesis, Technische Hochschule Darmstadt, Germany (1992).
10. B. Weigand and H. Beer, The morphology of ice structure in a parallel plate channel, *Proceedings of the Third International Symposium on Cold Regions Heat Transfer*, pp. 167–176. Fairbanks, AL (1991).
11. B. Weigand and H. Beer, Ice-formation phenomena for water flow inside a cooled parallel plate channel: an experimental and theoretical investigation of wavy ice layers, *Int. J. Heat Mass Transfer* **36,** 685–693 (1993).
12. S. Oiwake and H. Inaba, Freezing fracture of curved water pipes. *Bull. JSME* **29**(253), 2151–2155 (1986).
13. K. Ichimiya and R. Shimomura, Characteristics of ice formation in a curved channel containing flows—1. Unsteadiness of initial solidification and heat transfer at water–ice interface, *Heat Transfer Sci. Technol.*
14. S. Fukusako, Characteristics of freezing heat transfer in a 180 degree bend with a rectangular cross section, *Heat Transfer—Jap. Res.* **17**(4), 87–103 (1988).
15. P. Bradshaw, Effects of streamline curvature on turbulent flow, AGARDograph AG-169, Neuilly-sur-Seine, France (1973).
16. K. C. Muck, P. H. Hoffmann and P. Bradshaw, The effect of convex surface curvature on turbulent boundary layers, *J. Fluid Mech.* **161,** 347–369 (1985).
17. R. G. Deissler, Evolution of a moderately short turbulent boundary layer in a severe pressure gradient, *J. Fluid Mech.* **64,** 763–774 (1974).
18. R. G. Deissler, Evolution of the heat transfer and flow in moderately short turbulent boundary layers in severe pressure gradients, *Int. J. Heat Mass Transfer* **17,** 1079–1085 (1974).
19. P. M. Moretti and W. M. Kays, Heat transfer to a turbulent boundary layer with varying free-stream velocity and varying surface temperature—an experimental study, *Int. J. Heat Mass Transfer* **8,** 1187–1202 (1965).
20. R. Narasimha and K. R. Sreenivasan, Relaminarization of fluid flows, *Adv. Appl. Mech.* **19,** 248–264 (1979).
21. W. M. Kays, Heat transfer of a transpired boundary layer, JReport HMT-14, Thermo Sciences Division, Stanford University, U.S.A. (1971).
22. F. L. Wattendorf, A study of the effect of curvature on fully developed turbulent flow, *Proc. R. Soc. Lond.* **A148,** 565–598 (1934).
23. S. Eskinazi and H. Yeh, An investigation on fully developed flows in a curved channel, *J. Aeronautical Sci.* **23**(1), 23–34, 75 (1956).
24. M. Kobayashi *et al.*, Two-dimensional turbulent flow in a curved channel. *JSME Int. J. Ser.* II **32**(3), 324–331 (1989).
25. P. Bradshaw, T. Cebeci and J. Whitelaw, *Engineering Calculation Methods for Turbulent Flow*. Academic Press, London (1981).
26. J. Braun and H. Beer, The morphology of ice layers in curved rectangular channels, *Proceedings of the Fourth International Symposium on Thermal Engineering and Science for Cold Regions*, pp. 55–64. Hanover, NH (1993).
27. J. Braun, Konvektive Wärmeübertragung bei Erstarrungsvorgängen in durchströmten, gekrümmten Kanälen, Doctoral Thesis, Technische Hochschule Darmstadt, Germany (1994).
28. T. A. Reyhner and I. Flügge-Lotz, The interaction of a shock wave with a laminar boundary layer, *Int. J. Non-Linear Mech.* **3,** 173–199 (1968).